Interfacial behavior of confined mesogens at smectic-*C**–water boundary

Achu Chandran,[1,2,*] P. K. Khanna,[1] D. Haranath,[2,3] and Ashok M. Biradar[2,3]
[1]*Advanced Packaging Group, CSIR–Central Electronics Engineering Research Institute, Pilani 333031, India*
[2]*Academy of Scientific and Innovative Research, CSIR–National Physical Laboratory Campus, Dr. K. S. Krishnan Road, New Delhi 110012, India*
[3]*CSIR–National Physical Laboratory Campus, Dr. K. S. Krishnan Road, New Delhi 110012, India*

(Received 25 July 2017; revised manuscript received 16 January 2018; published 9 February 2018)

In this paper, we have investigated the behavior of mesogens at smectic-*C**–water interface confined in a liquid crystal (LC) cell with interfacial geometry. Polarized optical microscopy was used to probe the appearance of various smectic-*C** domain patterns at water interface owing to the reorientation of mesogens. The undulated stripe domains observed at the air interface of smectic-*C** meniscus vanished as the water entered into the smectic layers and focal conical domain patterns appeared at smectic-*C**–water boundary. A spatially variable electro-optical switching of LC molecules was also observed outside the electrode area of the interfacial cell. The electrode region at the interface, as well as on the water side, was damaged upon application of an electric field of magnitude more than 150 kV/m. The change in dielectric parameters of mesogens was extensively studied at interface after evaporating the water. These studies give fundamental insights into smectic-*C**–water interface and also will be helpful in fabricating better LC devices for electro-optical and sensing applications.

DOI: 10.1103/PhysRevE.97.022701

I. INTRODUCTION

Interdisciplinary research on liquid crystal (LC) interfaces is undergoing modern day renaissance because of its profound impacts on science, technology, industry, and medicine [1,2]. LCs are highly sensitive to external stimulus and surrounding events, which make them suitable candidate for interfacial studies. The applications based on LCs rely on the orientation control of mesogens at interface with surfaces and immiscible structures. The past decades have seen immense research activities on the display applications of LCs focusing on surface and geometrical confinement effects of LCs [3,4]. At present, researchers are exploring the dynamics of LCs at the interfaces with various surfaces and structures and its local effects for device applications such as LC-based biosensors, memory devices, and optical and photonic devices [5–7]. The interfacial studies on LCs with immiscible structures include dispersion of nano- and microsized particles in freely suspended and geometrically confined LCs [8–10], LC films at air-water interfaces [11–13], LC film-surfactant interactions [14], polymer-dispersed LC [15], etc.

Among the LC and other immiscible structures, the interfaces between anisotropic LCs with isotropic water and their dynamics are of fundamental and applied research interest. Various attempts to probe into the molecular arrangement, layering and wetting properties, and electro-optical switching of LC-water interfaces have been reported [16–20]. Most of the work in this area is carried out using conventional nematic LCs. The nematic LC-water interface enables the detection of biomolecular interactions in its vicinity by reorientation of mesogens. This makes them suitable candidates for LC based biosensors [21]. A method has been developed to transfer and organize microparticles at nematic LC-water interface using molecular ordering of LCs [22]. The temperature-dependent interfacial tension between water and nematic LCs in presence of adsorbed surfactants was measured by pendent drop method [11]. Harth *et al.* have measured the interfacial tension of a smectic LC in freely suspended film geometry in aqueous environment [23] and in surfactant solution [24].

Recently, an investigation on molecular arrangement and dynamics of geometrically confined ferroelectric mesogens in smectic-*C**–air interface revealed a homeotropic arrangement of mesogens at air boundary [25]. Reports on the dielectric and electro-optical studies of a ferroelectric LC (FLC)-water hybrid system prepared by mechanical mixing of water into the FLC host showed that the distribution of water in FLC is anisotropic [26]. The nematic-smectic phase transition of a thermotropic LC confined to a spherical shell and the dependency of its complex internal structure on director configuration were studied in detail [27,28]. Also, the tuning of defect configurations in nematic and smectic LC shells surrounded by aqueous phases is reported [29]. Iwashita *et al.* prepared stable, macroscopic, freely suspended smectic films in water with the help of a surfactant and observed a homeotropic anchoring of LC molecules at the film-water interfaces owing to the effect of surfactant molecules at interface [30]. The interfacial studies on geometrically confined smectic-*C** LC with water are rare due to the higher order and complexity of mesogens at chiral smectic phase and surface confinement effects. Also, the material properties, molecular arrangement, and reorientation of mesogens at smectic-*C**–water interface has been little-explored for device applications. This paper is an attempt to probe into the alignment and behavior of mesogens at smectic-*C**–water interface in a confined geometry.

*ac60369@gmail.com, achuchandran@ceeri.res.in

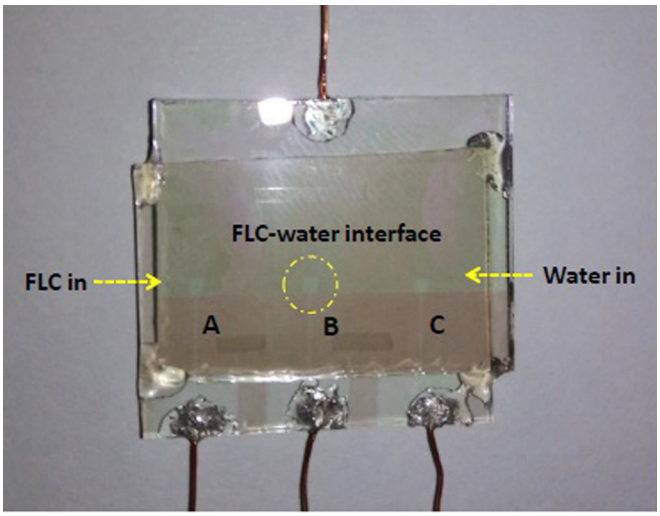

FIG. 1. Specially designed FLC-water interface cell before filling.

This paper presents a systematic study on the behavior of interfacial mesogens confined at smectic-C^*–water boundary in a LC cell geometry. The appearance of various domain patterns owing to the reorientation of LC molecules and spatially variable electro-optical switching is observed at smectic-C^*–water interface. The indium tin oxide (ITO) electrodes are burnt out in the water side of interfacial cells on application of high electric field. Also, the effect of water molecules on the dielectric parameters of the mesogens has been extensively studied. A comprehensive and precise understanding of smectic-C^*–water interface leads to the design and fabrication of better LC devices for electro-optical and sensing applications.

II. MATERIALS AND METHODS

A specially designed smectic-C^*–water interface geometry was used to investigate the molecular arrangement and dynamics of confined mesogens at water boundary. The electrode patterns were made on highly conducting (30 ohm/square) and optically transparent ITO-coated glass plates using photolithography. A strongly rubbed polymide layer of nylon 6/6 was coated on the patterned glass plates for homogeneous alignment of mesogens. The thickness of the sample cell was maintained as 20 μm using Mylar spacer. The fabricated interfacial cell before filling is shown in Fig. 1.

The FLC material used in this paper is LAHS-22 [31] and the phase sequence of the same is given as

$$\mathrm{Cry} \overset{(-3)-2\,^\circ\mathrm{C}}{\longleftrightarrow} \mathrm{Sm}C^* \overset{59\,^\circ\mathrm{C}}{\longleftrightarrow} \mathrm{Sm}A^* \overset{69\,^\circ\mathrm{C}}{\longleftrightarrow} \mathrm{iso}$$

where cry is the crystalline phase, SmC^* is the chiral smectic-C phase, SmA^* is the smectic-A phase, and iso is the isotropic phase.

The multielectrode system shown in Fig. 1 is well suited for interfacial studies, as it can act as three individual sample cells (A, B, and C) with identical cell parameters. The FLC material LAHS-22 is filled into the sample cell from the left side by capillary action (electrode A side) at isotropic temperature of the material. The filling is done in a controlled manner under polarizing optical microscope (POM) with parallel polarizers up to half (of electrode B) of the sample cell placed on a hot stage with a temperature controller. First, the empty cell with three electrode patterns (A, B, and C) was kept in a hot stage connected to a temperature controller. The hot stage was kept under POM and the temperature of the hot stage (i.e., sample cell) was raised to the isotropic temperature of FLC material, LAHS-22. Then a small amount of FLC material was kept at the opening side of the A electrode of the sample cell. The FLC material crept inside the cell by capillary action. When the FLC material reached half of the middle electrode (B electrode), which is seen under microscope, the temperature of the hot stage was cooled down slowly to room temperature. This prevents the further flow of FLC material, and phase transition from isotropic to smectic phases occurs. Upon cooling down the FLC to smectic-C^* phase, deionized (DI) water (electrical resistivity $\sim$18 M$\Omega\cdot$cm) was filled by the controlled capillary force, from the right side (electrode C side) of the sample cell, and a perfect interface was made in the middle of electrode B. A detailed probing into electrode B using various analytical tools gave insights into the molecular arrangement and dynamics of the smectic-C^*–water system, which is described in further sections.

The optical micrographs of the smectic-C^*–water interface system were taken with the help of POM (Axioskop-40, Carl Zeiss, Germany) fitted with a charge coupled device camera. The dielectric properties of the interface system were studied using an impedance analyzer (Wayne Kerr 6540 A, UK) in a frequency window of 20 Hz–1 MHz with a measuring peak to peak voltage of 0.5 V. A temperature controller (JULABO F-25 HE) was used for controlling the temperature with an accuracy of $\pm$0.1 °C for the experiment. While carrying out the temperature dependent studies, the sample holder containing the sample cell was kept thermally isolated from the external sources. The material parameters of mesogens, such as rotational viscosity and spontaneous polarization, were measured by using an automatic liquid crystal tester (Instec, USA). Contact angle measurement was done using the Drop Shape Analysis System (Model DSA10MK2 from Kruss GmbH, Germany).

III. RESULTS AND DISCUSSION

The appearance of various domain patterns owing to the arrangement of LC molecules inside the sample cell and the reorientation of the same in contact with water were investigated using POM. The images of the LC sample cell after filling the FLC material LAHS 22 up to midway of electrode B are shown in Fig. 2. As the material is cooled down to smectic-C^* phase (at 25 °C), a perfect smectic-C^*–air interface is formed inside the confined geometry before filling the water.

In Fig. 2(a), it is seen that mesogens are homogeneously aligned up to the air boundary. The boundary is seen as a dark line with a periodic stripe pattern towards the air side of interface. The dark line is due to the concave shape of FLC meniscus at air interface in a confined geometry, in which the light to observer is deflected [8]. The smectic undulation or periodic stripe pattern seen ahead of this dark line is quite interesting. A similar pattern is observed in the film thickness gradients or menisci regions of smectic free-standing films [32–36] and around the sufficiently large size inclusions on such films in smectic-C and smectic-A^* phases [10,37]. So

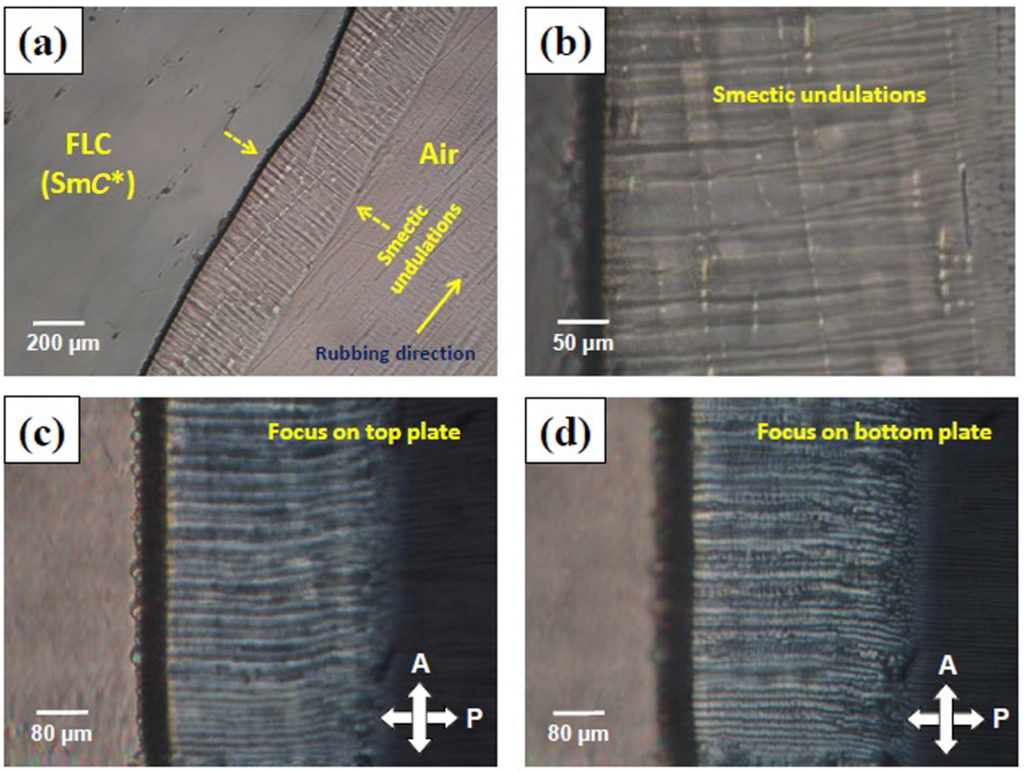

FIG. 2. POM images of (a) the LC interface sample cell on filling FLC material LAHS-22 up to half of the middle electrode (electrode "B"), making FLC-air interface with smectic undulation and stripe patterns near boundary. (b) Larger magnification of the smectic undulation and stripe patterns. The stripe patterns at (c) top plate and (d) bottom plate under crossed polarizers.

far, the physical origin of these striped patterns has not been revealed unambiguously. The spontaneously formed stripe patterns in smectic-*C** phase were initially interpreted as surface-splay domains owing to spontaneous surface polarization, which leads to *c*-director splay at the surfaces [38]. It has also been interpreted as a result of layer shrinkage and bookshelf anchoring of the film at the outer substrate during the smectic-*A*–smectic-*C** phase transition [32]. It is observed that the stripe domain is a geometrical feature formed in the regions of film thickness gradient and the direction of stripe is parallel to the gradient [33]. In Fig. 2(b), the smectic undulation and stripe domain patterns are clearly visible under better magnification. As the interface cell has two parallel glass plates confining the mesogens in a sandwich manner, two FLC films with thickness gradient are formed at the air interface inside the cell (on top and bottom plates). The stripe domains seen in both films at smectic-*C** phase are clearly distinguishable as the microscope is focused on top [Fig. 2(c)] and bottom [Fig. 2(d)] plates separately with crossed polarizers.

In order to form smectic-*C**–water interface at electrode B, the DI water is filled from the electrode C side using capillary action. Figure 3 illustrates the formation of smectic-*C**–water interface, electro-optical switching of mesogens, and its dynamics at water boundary.

It is seen from Fig. 3(a) that the homogeneous alignment of mesogens in the interface region is disturbed as the water penetrates into the LC layers. On comparing Figs. 2(a) and 3(a), a noticeable decrease in the width of the dark line in the interface region is observed owing to the reduction in the curvature of the LC boundary region. Also, the stripe domain patterns seen in the smectic meniscus of upper and lower glass plates are also swept out on water diffusion. Interestingly, focal conical domain (FCD) patterns are formed in the smectic-*C**–water interface region as shown in Figs. 3(b) and 3(c) [marked in square and magnified in the inset of Fig. 3(b)] confirming the molecular reorientation at the boundary. The FCDs are formed in smectic LCs owing to the antagonistic boundary conditions of the film surface [25], i.e., the planar alignment on the substrate surface and the homeotropic (perpendicular) alignment at the interface region or vice versa [39]. Reports on LC-water interface infer that mesogens have a tendency to align planar with water boundary [40] and it aligns homeotropically at air interface [25,39]. Here, as water molecules penetrate the FLC interface region replacing the air during the capillary filling process, the mesogens which are homeotropically aligned with respect to air interface reorient to planar with water interface. The mechanism of molecular reorientation is clearly illustrated in the schematic (Fig. 4).

A schematic depiction of smectic-*C**–water interface before filling water and in presence of water is made in Fig. 4. In Fig. 4(a), smectic-*C**–air interface is shown in which the mesogens are sandwiched in between ITO-coated glass plates with strongly rubbed polymide layers.

The mesogens are aligned planar in smectic layers. The concave smectic-*C**–air interface with LC molecules contributing to smectic undulation pattern (stripe domain) at smectic-*C**–air boundary is marked in Fig. 4(a). When water molecules are introduced into the interface region replacing air,

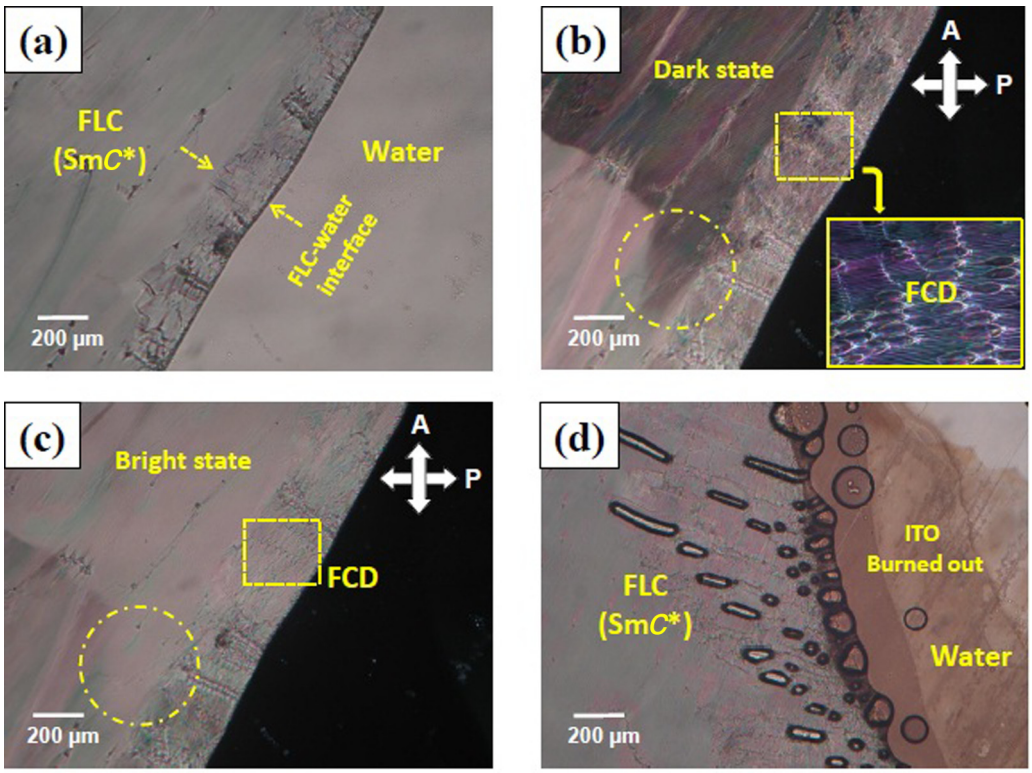

FIG. 3. POM images showing (a) the formation of FLC-water interface with reorientation of mesogens at interface region marked. Electro-optical switching of LC molecules showing (b) dark state and (c) bright state of FLC on application of ac bias of 2 V_{pp} (electric field: 100 kV/m) under crossed polarizers. (d) Burnout of ITO electrodes at ac bias of >3 V_{pp} (electric field: 150 kV/m). The inset of (b) shows the appearance of FCD pattern.

a reorientation of interfacial mesogens is seen [Fig. 4(b)]. The curvature of interface region is reduced and the LC molecules which were oriented perpendicular with respect to air interface

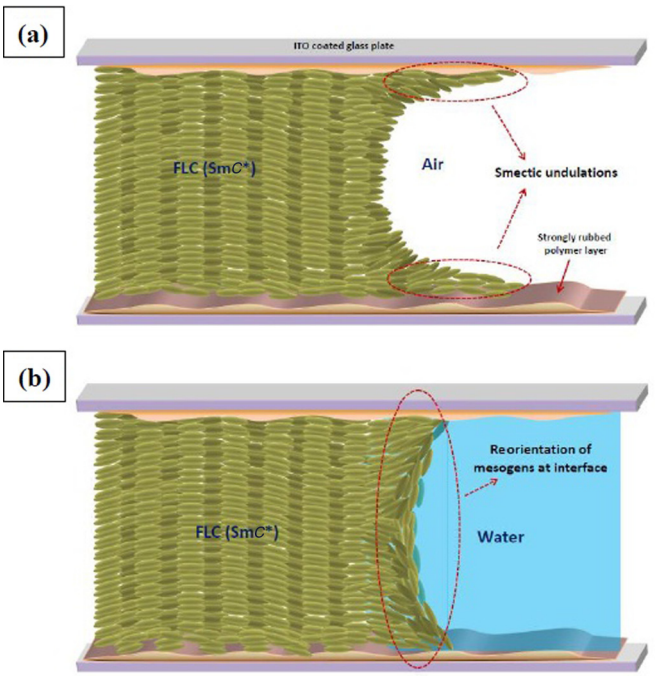

FIG. 4. Schematic depiction of (a) FLC-air interface and (b) FLC-water interface in a confined geometry.

attained a planar orientation with water molecules. Thus an antagonistic boundary condition occurred at smectic-*C**–water interface, which appeared as FCD structure.

When an ac bias field of 2-V_{pp} magnitude (electric field: 100 kV/m) and 1-Hz frequency is applied to the smectic-*C**–water interface region, switching of mesogens in dark and bright state is seen in the FLC region of the interface electrode as shown in Figs. 3(b) and 3(c), respectively. Here, in both figures, in addition to the conventional switching mechanism, a spatially variable electro-optical switching of mesogens [19,26] is also seen outside the electrode area near the interface region [marked inside circle in Figs. 3(b) and 3(c)]. This spatially variable switching is a result of diffusion of water into smectic layers and the interaction of curved electric field just outside of the electrode area with the mesogens of the water-diffused region [19]. As the magnitude of electric field was further increased to 3 V_{pp}, the electro-optical switching was strengthened and beyond 3 V_{pp} (electric field: >150 kV/m) the ITO electrodes suddenly burnt out as shown in Fig. 3(d). It is reported that under a high electric field an ionic current path with high current density is created between ITO electrodes which decomposed the ITO into indium, tin, and oxygen and is seen as being dark in color [41]. Here, the ions in water have contributed to the high current density conductive path between the ITO patterns and the burning out of ITO by joule heat. As a result of this localized heating on ITO electrodes with water in confined geometry, some water was evaporated leaving gas bubbles near the interface region. It is interesting to see the shape of gas bubbles in water side and FLC side

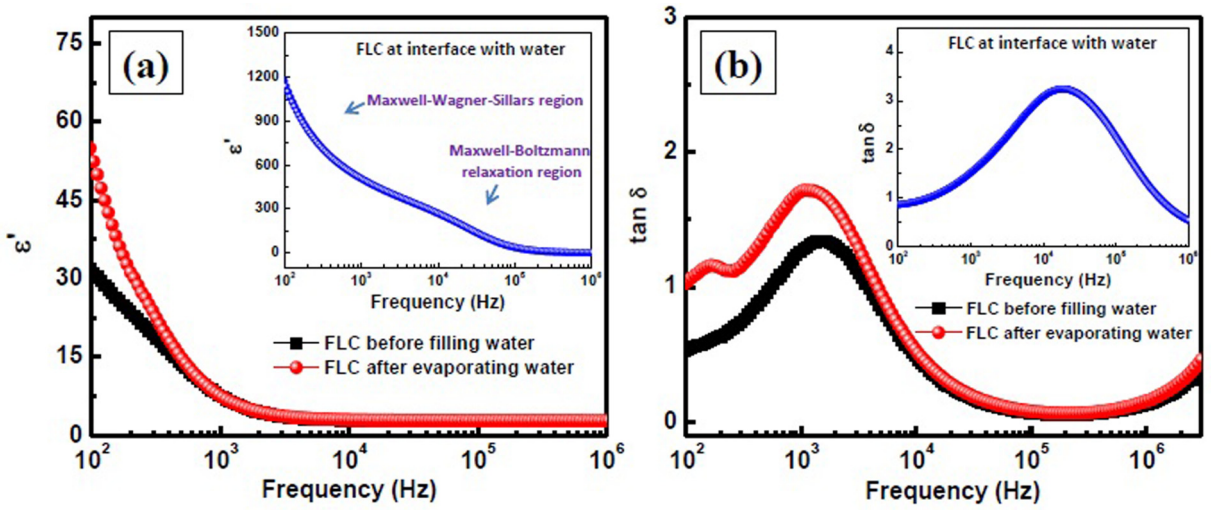

FIG. 5. Dielectric (a) dispersion (ε' vs log of frequency) and (b) absorption (tan δ vs log of frequency) spectra of FLC-water interface before filling water, in presence of water (inset) and after evaporating water at room temperature (25 °C).

[Fig. 3(d)]. Gas bubbles in water side are spherical in shape due to surface tension and are elongated in FLC side owing to the layer structure of FLCs.

Since the ITO region at smectic-C*–water interface was burnt out, the sample could not be used for further studies. A fresh smectic-C*–water interface sample was prepared for dielectric and material parameter studies. Dielectric spectroscopy is a versatile tool for probing various dielectric relaxation processes in a material [25]. In order to study the effect of water molecules on the dielectric relaxation process of FLCs at interface in a confined geometry, dielectric dispersion (ε' versus log of frequency) and absorption spectra (dielectric loss factor, tan δ, versus log of frequency) are taken before filling water, in presence of water and after evaporating water as shown in Fig. 5.

Figure 5(a) shows the dielectric dispersion spectrum of smectic-C*–water interface, where dielectric permittivity (ε') of the sample is plotted against frequency, before filling water, in presence of water [inset of Fig. 5(a)], and after evaporating water at room temperature (25 °C). From Fig. 5(a), it is seen that the ε' value of mesogens with air interface (before filling water) is ∼30 at 100 Hz. As the water is introduced into the interface cell, it is interesting to see that the ε' value of smectic-C*–water interface increases tremendously, i.e., almost 30 times that of smectic-C*–air interface at 100 Hz [inset of Fig. 5(a)]. It is well known that a water molecule can autodissociate into H^+ and OH^- ion pairs [42,43]. When an alternating electric field is applied to water sandwiched between electrodes with a frequency sweep, different dielectric processes can occur. At low frequencies, the dipolar water molecules get aligned with the direction of electric field and the ions move towards the opposite electrodes owing to a phase difference between the electrodes (Maxwell-Wagner-Sillars phenomenon) [44]. Thus, the ionic effect is more dominant at low frequencies imparting a large jump in ε' value, even if ion pairs are lesser in number than water molecules [44–46]. At high frequencies, the ion pairs are unable to follow the electric field as the polarity of electrodes changes quickly. Only water molecules are able to respond effectively at high frequency and the ε' value follows Maxwell-Boltzmann statistics [45]. Now, the water inside the interface cell was allowed to evaporate and the dielectric spectrum of smectic-C*–air interface was taken after 48 h. From Fig. 5(a), it is seen that the dielectric dispersion spectrum is almost restored as that of fresh smectic-C*–air interface with a small increment in ε' value (∼50 at 100 Hz). This small increment is due to the traces of entrapped ion species inside FLC layers from water diffusion. The presence of ionic traces is clearly evident in the dielectric absorption spectrum. Figure 5(b) shows the dielectric absorption spectrum (tan δ versus frequency) of smectic-C*–water interface before filling water, in presence of water [inset of Fig. 5(b)], and after evaporating water at room temperature (25 °C). In Fig. 5(b), it is seen that before filling water into smectic-C*–air interface only

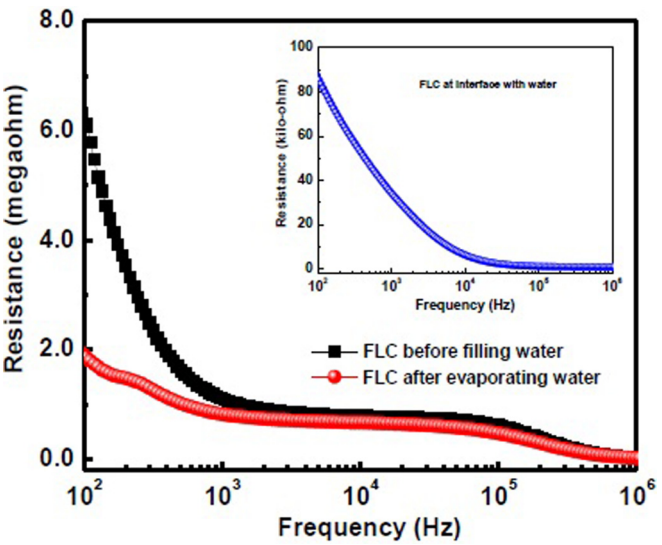

FIG. 6. Resistance vs log of frequency of FLC-water interface before filling water, in presence of water (inset) and after evaporating water at room temperature (25 °C).

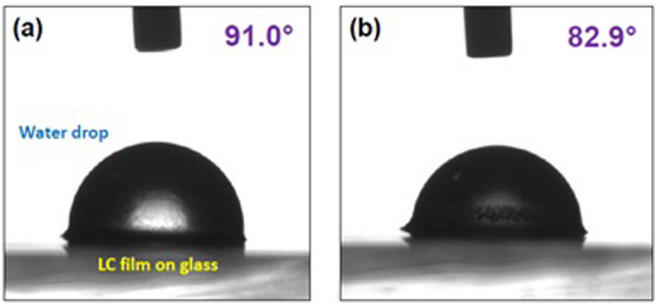

FIG. 7. The contact angle measured between FLC film and water droplet just after (a) 5 s and (b) 5 min of dropping the water.

Goldstone mode relaxation at a frequency of ∼1 kHz is present in mesogens owing to the phase fluctuation in the azimuthal orientation of the director [47]. But after evaporating water, an additional peak is seen [Fig. 5(b)] in the low frequency region (∼150 Hz) due to ionic species from water contained in FLC layers [44,45].

In order to confirm the presence of ions even after evaporation of water, resistance of the smectic-*C**–water interface cell is measured with frequency before filling water, in presence of water (inset of Fig. 6), and after evaporating water at room temperature (25 °C) as shown in Fig. 6.

From Fig. 6, it is seen that the resistance of smectic-*C**–air interface (before filling water) is ∼6 MΩ at 100 Hz. When water is introduced into the interface cell, the resistance suddenly dropped to ∼85 kΩ due to the ionic conductivity of water (inset of Fig. 6). As the water was evaporated and the resistance of interface was checked after 48 h, it is seen that the value of resistance is restored to ∼2 MΩ. From Fig. 6, it is clear that some ionic species are still trapped in between FLC layers which are hindering the full restoration of resistance value.

In order to estimate the FLC-water interface tension, a drop of water was placed over the FLC film supported on glass substrate. The contact angle between water and FLC film was measured just after 5 s and 5 min of dropping the water as shown in Fig. 7.

It is clearly seen from Fig. 7 that the LC slowly creeps up the droplet's surface, thus leading to a change of contact angle.

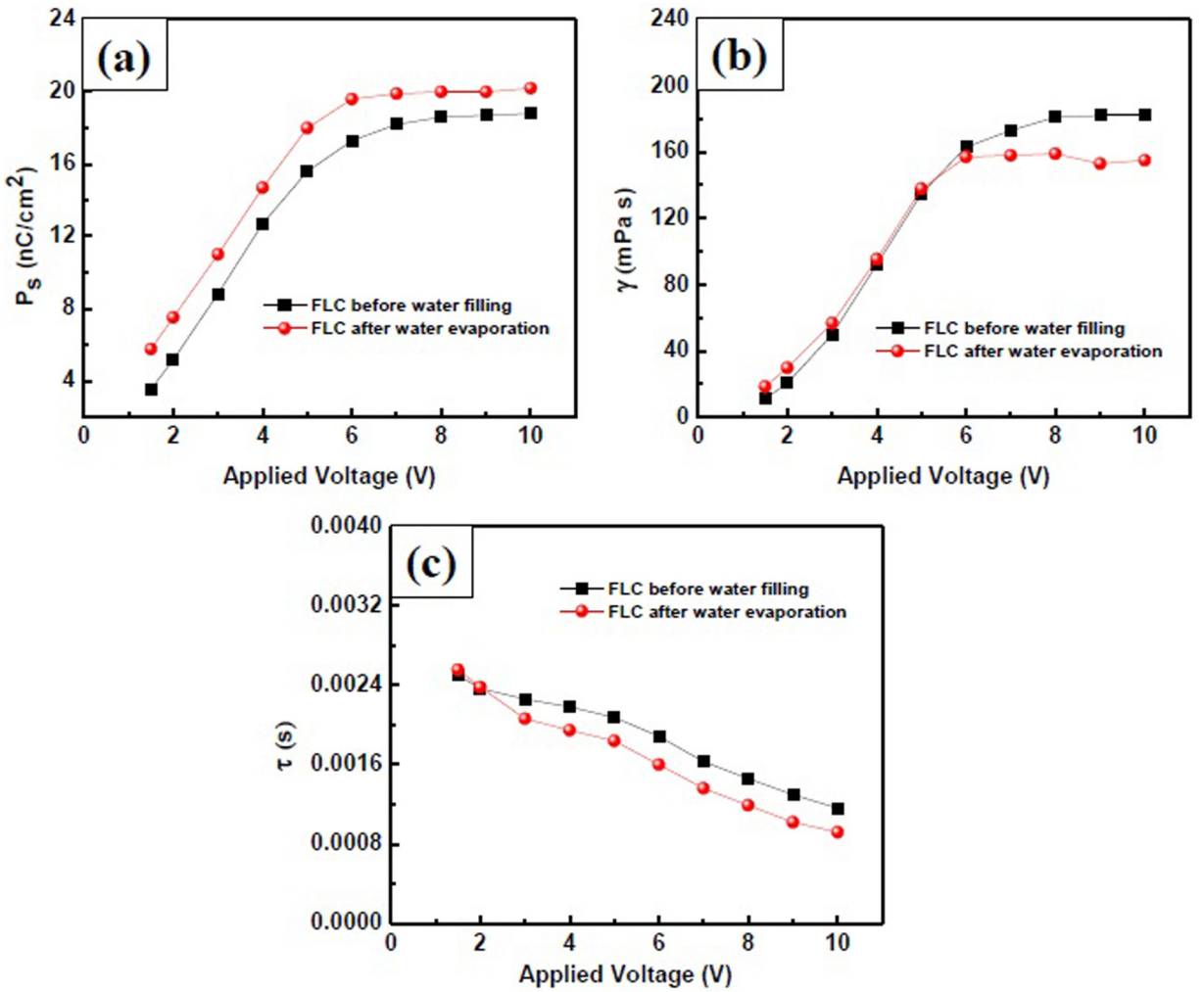

FIG. 8. Material parameters of FLC. (a) Spontaneous polarization. (b) Rotational viscosity. (c) Response time with applied voltage before filling water and after evaporating water at room temperature (25 °C).

This phenomenon is purely due to the interfacial tensions at the contact line. The interface tension of FLC-water interface can be determined using Young's equation [Eq. (1)]:

$$\sigma_{\mathrm{FLC}} = \sigma_{\mathrm{FLC}-W} + \sigma_W \cos(\theta) \quad (1)$$

where σ_{FLC} is the surface tension of ferroelectric liquid crystals, $\sigma_{\mathrm{FLC}-W}$ is the interface tension of FLC-water boundary, σ_W is the surface tension of water (72.8 mN/m at 25 °C), and θ (91° from Fig. 7) is the contact angle between water and FLC film. Since the exact value of surface tension of the FLC material, LAHS 22, is not known, let us consider it as ∼21 mN/m [48]. Substituting the values in Eq. (1), the interface tension value of FLC-water interface is ∼22.27 mN/m.

The variations in the material parameters of mesogens were also investigated before filling and after evaporation of water and are given in Fig. 8.

From Fig. 8, it is seen that the variation in material parameters of FLC is very small due to interface with water and its subsequent evaporation. Since the saturation value of material parameters appeared at an applied voltage of ∼7 V (Fig. 8), the measurement in presence of water is not possible due to burning out of ITO electrodes as seen in Fig. 3(d). As seen in Fig. 8(a), the saturation value of spontaneous polarization (P_s) of mesogens before filling water is ∼18.5 nC/cm^2, and after 48 h of water evaporation the P_s value has slightly increased to ∼20 nC/cm^2 due to the traces of ion pairs from water in between FLC layers [44,45]. Also, these trapped ions and water molecules in between mesogens are responsible for the decrement in the saturation value of rotational viscosity (γ) of FLC as shown in Fig. 8(b). The increase in P_s and decrease in γ have resulted in a slightly faster response time (τ) of mesogens after water evaporation [Fig. 8(c)] as P_s, γ, and τ are related as illustrated in Eq. (2):

$$\tau = \gamma/(P_s E) \quad (2)$$

where τ is response time, γ is the rotational viscosity, P_s is the spontaneous polarization, and E is the applied electric field, respectively.

IV. CONCLUSION

This paper focuses on the molecular arrangement and behavior of geometrically confined mesogens at smectic-C^*–water interface in a newly designed LC cell. The undulated stripe domains at the air interface of confined smectic-C^* films and the appearance of focal conical domain patterns at smectic-C^*–water boundary owing to the reorientation of interfacial mesogens were probed using POM. A spatially variable electro-optical switching of LC molecules was observed outside the electrode area of the interfacial cell. On application of an electric field of magnitude more than 150 kV/m, the ITO electrodes on the water side burnt out due to the creation of a high current intensity conductive path of ions in water. The change in dielectric parameters of smectic-C^* LC at water interface was also studied after evaporating water. This paper reveals insights into the smectic-C^*–water interfacial system and will be helpful in designing advanced LC-based devices for novel applications.

ACKNOWLEDGMENTS

The authors sincerely thank the Director, CSIR–Central Electronics Engineering Research Institute for his sustained encouragement and support. The authors acknowledge Dr. Tilak Joshi and Dr. Amit Choudhary for the fruitful discussions.

[1] S. J. Woltman, G. D. Jay, and G. P. Crawford, Nat. Mater. **6**, 929 (2007).
[2] J. Prakash, A. Chandran, and A. M. Biradar, Rep. Prog. Phys. **80**, 016601 (2017).
[3] T. Geelhaar, Liq. Cryst. **24**, 91 (1998).
[4] N. A. Clark and S. T. Lagerwall, Appl. Phys. Lett. **36**, 899 (1980).
[5] M. Tyagi, A. Chandran, T. Joshi, J. Prakash, V. V. Agrawal, and A. M. Biradar, Appl. Phys. Lett. **104**, 154104 (2014).
[6] A. Chandran, J. Prakash, J. Gangwar, T. Joshi, A. K. Srivastava, D. Haranath, and A. M Biradar, RSC Adv. **6**, 53873 (2016).
[7] H. Ren, Y.-H. Fan, and S.-T. Wu, Appl. Phys. Lett. **83**, 1515 (2003).
[8] A. Jakli, B. Senyuk, G. Liao, and O. D. Lavrentovich, Soft Matter and Supplementary Material (ESI) **4**, 2471 (2008).
[9] A. Chandran, J. Prakash, P. Ganguly, and A. M. Biradar, RSC Adv. **3**, 17166 (2013).
[10] C. Bohley and R. Stannarius, Soft Matter **4**, 683 (2008).
[11] J-W Kim, H. Kim, M. Lee, and J. J. Magda, Langmuir **20**, 8110 (2004).
[12] L. Zou, J. Wang, P. Basnet, and E. K. Mann, Phys. Rev. E **76**, 031602 (2007).
[13] Y. Bai and N. L. Abbott, Langmuir **27**, 5719 (2011).
[14] Ch. Bahr, Phys. Rev. Lett. **99**, 057801 (2007).
[15] J. W. Doane, N. A. Vaz, B. G. Wu, and S. Žumer, Appl. Phys. Lett. **48**, 269 (1986).
[16] G. P. Crawford, R. J. Ondris-Crawford, J. W. Doane, and S. Zumer, Phys. Rev. E **53**, 3647 (1996).
[17] A. M. Somoza, L. Mederos, and D. E. Sullivan, Phys. Rev. Lett. **72**, 3674 (1994).
[18] Ch. Bahr, Phys. Rev. E **73**, 030702 (2006).
[19] A. Choudhary, I. Coondoo, J. Prakash, K. Sreenivas, and A. M. Biradar, Appl. Phys. Lett. **94**, 174101 (2009).
[20] A. Chandran, T. Joshi, P. K. Khanna, D. S. Mehta, D. Haranath, and A. M. Biradar, J. Appl. Phys. **122**, 014101 (2017).
[21] W. Iglesias, N. L. Abbott, E. K. Mann, and A. Jakli, ACS Appl. Mater. Inter. **4**, 6884 (2012).
[22] I-H. Lin, G. M. Koenig, Jr., J. J. de Pablo, and N. L. Abbott, J. Phys. Chem. B **112**, 16552 (2008).
[23] K. Harth and R. Stannarius, Phys. Chem. Chem. Phys. **15**, 7204 (2013).
[24] K. Harth, L. M. Shepherd, J. Honaker, and R. Stannarius, Phys. Chem. Chem. Phys. **17**, 26198 (2015).
[25] A. Chandran, A. Choudhary, P. Singh, D. Haranath, and A. M. Biradar, Soft Matter **11**, 749 (2015).
[26] G. Singh, A. Choudhary, G. Vijaya Prakash, and A. M. Biradar, Phys. Rev. E **81**, 051707 (2010).

[27] T. Lopez-Leon, A. Fernandez-Nieves, M. Nobili, and C. Blanc, Phys. Rev. Lett. **106**, 247802 (2011).
[28] H-L. Liang, S. Schymura, P. Rudquist, and J. Lagerwall, Phys. Rev. Lett. **106**, 247801 (2011).
[29] H-L. Liang, J-H. Noh, R. Zentel, P. Rudquist, and J. P. F. Lagerwall, Phil. Trans. R. Soc. A **371**, 20120258 (2013).
[30] Y. Iwashita, S. Herminghaus, R. Seemann, and C. Bahr, Phys. Rev. E **81**, 051709 (2010).
[31] S. Tripathi, J. Prakash, A. Chandran, T. Joshi, A. Kumar, A. Dhar, and A. M. Biradar, Liq. Cryst. **40**, 1255 (2013).
[32] J. C. Loudet, P. V. Dolganov, P. Patricio, H. Saadaoui, and P. Cluzeau, Phys. Rev. Lett. **106**, 117802 (2011).
[33] K. Harth, A. Eremin, and R. Stannarius, Ferroelectrics **431**, 59 (2012).
[34] K. Harth, B. Schulz, C. Bahr, and R. Stannarius, Soft Matter **7**, 7103 (2011).
[35] R. Stannarius, A. Eremin, and K. Harth, Liq. Cryst. **44**, 1201 (2017).
[36] M. Selmi, J.-C. Loudet, P. V. Dolganov, T. Othman, and P. Cluzeau, Soft Matter **13**, 3649 (2017).
[37] K. Harth and R. Stannarius, Eur. Phys. J. E **28**, 265 (2009).
[38] R. B. Meyer and P. S. Pershan, Solid State Commun. **13**, 989 (1973).
[39] W. Guo and C. Bahr, Phys. Rev. E **79**, 061701 (2009).
[40] P. Popov, E. K. Mann, and A. Jákli, Phys. Rev. Appl. **1**, 034003 (2014).
[41] J. He, M. Lu, X. Zhou, J. R. Cao, K. L. Wang, L. S. Liao, Z. B. Deng, X. M. Ding, X. Y. Hou, and S. T. Lee, Thin Solid Films **363**, 240 (2000).
[42] B. L. Trout, and M. Parinello, Chem. Phys. Lett. **288**, 343 (1998).
[43] T. Yagasaki, I. Iwahashi, S. Saito, and I. Ohmine, J. Chem. Phys. **122**, 144504 (2005).
[44] H. Jansson, R. Bergman, and J. Swenson, Phys. Rev. Lett. **104**, 017802 (2010).
[45] A. Angulo-Sherman and H. Mercado-Uribe, Chem. Phys. Lett. **503**, 327 (2011).
[46] A. Chandran, J. Prakash, T. Joshi, and A. M. Biradar, J. Mol. Liq. **198**, 280 (2014).
[47] A. M. Biradar, S. Wrobel, and W. Haase, Phys. Rev. A **39**, 2693 (1989).
[48] H. Schüring, C. Thieme, and R. Stannarius, Liq. Cryst. **28**, 241 (2001).